Materials Today Communications 22 (2020) 100831

Contents lists available at ScienceDirect

Materials Today Communications

journal homepage: www.elsevier.com/locate/mtcomm

Effect of substitutional Cu atoms on the electronic and optical properties of KCl: A DFT approach

Roberto Núñez-González[a,*], R. Aceves[b,*], José Luis Cabellos[b], Alvaro Posada-Amarillas[b]

[a] Departamento de Matemáticas, Universidad de Sonora, Blvd. Luis Encinas y Rosales S/N, 83000 Hermosillo, Sonora, México
[b] Departamento de Investigación en Física, Universidad de Sonora, Blvd. Luis Encinas y Rosales S/N, 83000 Hermosillo, Sonora, México

ABSTRACT

The electronic and optical properties of KCl and Cu doped KCl (KCl:Cu) were calculated within full potential augmented plane wave method based on Density Functional Theory (DFT), as implemented in WIEN2k software. Calculations were carried out using two energy functional approximations, the exchange-correlation functional of Perdew, Burke and Ernzerhof (PBE96) to optimize the KCl lattice parameter, and the modified Becke-Johnson (mBJ) exchange potential in combination with the local density approximation (LDA) for correlation, to obtain the band structure. The energy bands reveal the insulating properties of KCl with a direct band gap of 8.6 eV, and the semiconductor nature of KCl:Cu with a direct band gap of 3.4 eV. From the analysis of the total and partial density of states, it is apparent that the KCl and KCl:Cu states at the Fermi level arise from Cl *p* states and Cu *d* states, respectively. Also, the optical properties reported here (dielectric function and absorption spectra) show that Cu atoms are responsible of electronic excitations occurring from Cu *d* valence bands to conduction bands of Cu, Cl and K with *p* character.

1. Introduction

Optical properties of monovalent copper as dopant in alkali halide (HA) crystals havebeen the subject of a variety of experimental and theoretical studies since the decade of the 1970's due to its remarkable properties of absorption (UV) and emission (UV–vis) of light, characteristics that make these crystals excellent phosphor materials for a number of technological applications. In copper-doped HA crystals, the presence of several absorption bands in the UV region has been reported, assigning these bands the inner electronic transition $3d^{10}\rightarrow 3d^{9}4s^{1}$ of isolated copper [1]. Several theoretical studies based on different approaches have supported this result [2,3]. However, the high oscillator strength as well as the temperature dependence of the absorption intensity shown in some HA has introduced a controversy, stimulating some authors to ascribe this absorption to the allowed electronic transition $3d^{10}\rightarrow 3d^{9}4p^{1}$ of the isolated copper ions [4]. In fact, W. E. Hagston [5] (and references therein) suggests as an alternative explanation for KCl, that the forbidden electronic transition $3d^{10}\rightarrow 3d^{9}4s^{1}$ occurs with the Cu^{+} ions located in an off-center position. This possibility is strongly supported by the work carried out by Stephen A. Pyne [6], who studied the off-center effect on the components of the $3d^{10}\rightarrow 3d^{9}4s^{1}$ transition of Cu^{+} ions in HA by using the crystal-field theory, and also through studies on the optimal position of substitutional Cu^{+} in KCl crystals reported by Furuya et al. [7].

The fast growing of the medical diagnostics technology, e.g. nuclear medicine and computer imaging, stimulated during the past decade an intensive research effort to find new Cu^{+}-doped matrices to detect ionizing radiation (X-ray, gamma and beta rays, protons) through luminescence measurements, *i.e.*, thermoluminescence (TL) and optically stimulated luminescence (OSL) [8–14]. In recent studies, copper-doped single $LiGaO_2$ [8] and alkali halo-phosphato $Na_2Zn(PO_4)Cl$ [9] crystals showed green and blue luminescence under UV excitation, respectively, property that is favorable to convert them in phosphor materials and usable as radiation sensors. In these crystals, the UV absorption signal has been attributed to both inner transitions, $3d^{10}\rightarrow 3d^{9}4s^{1}$ and $3d^{10}\rightarrow 3d^{9}4p^{1}$, of the isolated Cu^{+} ions.

Recently, several studies have been performed to analyze the effect of X-ray [10,11], γ-ray [11], and also UV radiation [12], in Cu^{+}-doped silica glasses (SiO_2) obtained by sol-gel method in shape of monolith as well as optical fiber, for the development of real time and remote dosimetry to observe the radiation effects in dangerous locations or places difficult to access. Also, investigations of Cu-doped amorphous silica-glass optical fiber were conducted to analyze its potential use in proton-therapy treatments by OSL methodology [13]. For UV radiation monitoring, several materials have been studied due to their potential use as TL and OSL dosimeters. Copper-doped silica glass optical fiber [12] and ZrO_2:Cu^{+} nanocrystalline [14] were also analyzed under UV radiation, and KCl:Eu^{2+} crystals were tested for monitoring radiation harmful to health [15,16]. In the latter, the TL and OSL signals were related to an ionizing effect of the Eu^{2+} impurities.

* Corresponding authors.
E-mail addresses: ronunez@mat.uson.mx (R. Núñez-González), raceves@cifus.uson.mx (R. Aceves).

https://doi.org/10.1016/j.mtcomm.2019.100831
Received 21 October 2019; Accepted 5 December 2019
Available online 06 December 2019
2352-4928/ © 2019 Elsevier Ltd. All rights reserved.

TL and OSL are phenomena based on the existence of electrons and holes produced during the irradiation process. UV dosimetry in copper-doped fused quartz glass suggests the excited states of Cu^+ should be close to the conduction band, hence expecting mixing between these states to produce free electrons and holes (like Cu^{2+}) that may be trapped in metastable traps. Afterwards, electrons and holes can recombine via photo- or thermal-stimulation to produce OSL or TL signals, respectively [17]. On the contrary, under ionizing radiation, for instance X-rays, in Cu-doped $LiAlO_2$ [18] or in KCl:Cu^+ [19], where it is believed the excited state of Cu^+ is well separated from the conduction band and the mixing effect of the excited state should not be observed, the OSL spectra in both crystals notably coincide with the photoluminescence (PL) of the inner transitions of Cu^+.

Theoretically, structural, electronic and optical properties of pure and Cu^+-doped HA have been recently studied in the Density Functional Theory (DFT) formalism [20–22]. The pressure-dependent electronic properties in pure KCl have been investigated through *ab initio* calculations based on the pseudopotential approach with the DFT method [20]. Calculations in the rocksalt structure of KCl revealed that the valence band is formed by Cl 3*s* and Cl 3*p* orbitals and also by K 3*p* orbitals, but the lower part of the conduction band is dominated by K 3*s* orbitals [20]. In Cu^+-doped LiF and NaF crystals, the energy of the $3d^{10}\rightarrow 3d^9 4s$ and $3d^{10}\rightarrow 3d^9 4p$ transitions was obtained and their absorption spectra determined, employing a simple model of oscillator strength [21]. These calculations were performed on the model cluster $M_{12}F_{14}Cu^+$ (M = Li, Na; F = Fluorine) utilizing the embedded-cluster approach to electronic structure calculations in crystals. The Cu^+ ion was placed in the center of clusters. In this approach, the energy difference between both inner transitions of Cu^+ was about 3.2 and 2.5–3.0 eV in NaF:Cu^+ and LiF:Cu^+, respectively. Additionally, the obtained absorption spectrum showed two bands that were associated with the splitting of the $3d^9$ level of the $3d^{10}\rightarrow 3d^9 4s^1$ transition of copper ions due to the crystalline field [21]. Formerly, the electronic structure and optical properties of LiF:Cu^+ were calculated by the DFT scheme using the plane-wave pseudopotential approach [22]. In that study the results revealed the presence of the Cu 3*d* level inside the band gap due to Cu^+ doping of LiF. In this crystal compound it was also determined that the Cu *s* and *p* electronic levels are close or mixed with the states of the conduction band of LiF crystals.

Clearly, in spite of the remarkable efforts that have been made to understand the origin of the absorption and emission electronic transitions observed in crystalline matrices doped with Cu ions, up to date this is an objective not fully reached and additional studies are evidently required. In this work, we investigated the effect of Cu doping in the KCl crystal by performing first principles calculations of the optical properties of KCl and KCl:Cu crystals. For these calculations we assume the Cu ions substitute K ions, considering copper static and placed on-center. The lattice deformation is taken into account considering the difference in the ionic radii of Cu and K ions. This paper is organized as follows: In Section 2 we give the computational details of this work, Section 3 presents a detailed discussion of results, and conclusions are provided in Section 4.

2. Structural and computational details

Potassium Chloride (KCl) is a typical ionic crystal with rock salt-type structure (NaCl). The experimental lattice parameter of this face-centered cubic (fcc) crystal is a = 6.29 Å and the associated space group is Fm-3 m (number 225) [23]. The cation atom (K) is located at (0, 0, 0), while the anion atom (Cl) is at position (1/2, 1/2, 1/2) within the primitive unit cell. In the current work, the optimum lattice parameter is obtained by periodically varying the unit cell volume from the experimentally known data, calculating at each step the corresponding DFT energy. To model the KCl:Cu structure, we use a cubic 3 × 3 × 3 supercell from the previously obtained KCl optimized cell, replacing one of the K atoms in the supercell by a Cu atom. Fig. 1 depicts the supercell thus generated, displaying the large distance between Cu atoms. In order to optimize the atomic positions and lattice parameter of this KCl:Cu supercell, we first carried out an internal relaxation of the atomic positions, then we calculated the total energy as a function of the cell volume to obtain the optimized lattice parameter. The resulting optimized cells for both KCl and KCl:Cu were utilized to calculate the electronic and optical properties of the pristine and Cu-doped crystals.

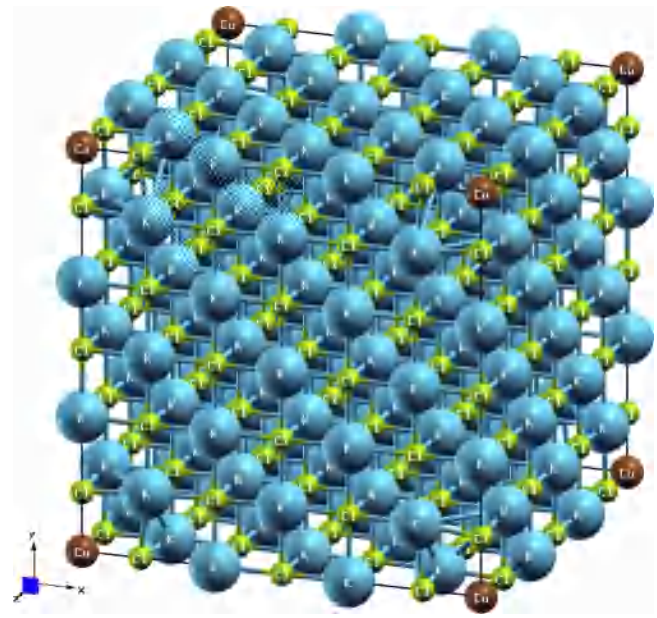

Fig. 1. Cubic 3 × 3 × 3 supercell model for KCl:Cu. Blue, green, and brown spheres represent K, Cl, and Cu atoms, respectively. (For interpretation of the references to colour in this figure legend, the reader is referred to the web version of this article).

The calculation of the electronic and optical properties of KCl and KCl:Cu was performed using a relativistic "full-potential" method based on "augmented-plane waves + local orbitals" (APW + lo) [24] within the DFT scheme [25,26], as implemented in the WIEN2k code [27]. In the APW method the unit cell volume is partitioned in two regions: muffin tin spheres (around each nucleus) and interstitial region. Inside each atomic sphere the wave function is approximated by a linear combination of radial functions times spherical harmonics, while in the interstitial region a plane wave expansion is used. For the exchange-correlation energy functional we employed two approximations: a generalized gradient approximation (GGA) to the exchange-correlation energy functional in the parametrization of Perdew, Burke and Ernzerhof (PBE96) [28], and the combination of the modified Becke-Johnson for exchange potential (mBJ) [29,30] together with the LDA approximation to the correlation [26]. The mBJ potential is a modification of the exchange potential of Becke and Johnson (BJ) [31], which reproduces the experimental gap of semiconductors with accuracy several orders of magnitude better than the previous version of the WIEN2K code using either the LDA or the GGA approximations, and is computationally cheap and efficient. For an extensive presentation and analysis of mBJ potential, see Koller et al. [30]. The computational implementation of mBJ approximation has three free parameters, which can be selected when starting the calculations. Specifically, in our work we use the parameterization presented by Tran and Blaha [29] (A = -0.012, B = 1.023 $bohr^{1/2}$, and e = 0.5).

The maximum l value for the waves inside the atomic sphere was set to l_{max} = 10. The muffin tin radii R_{mt} was set to 2.5 a.u. (atomic units) for potassium, chlorine and copper atoms. The wave function in the interstitial region was expanded in plane waves with a cutoff of K_{max} = $7.5/R_{mt}$ for KCl and K_{max} = $7.0/R_{mt}$ for KCl:Cu, while the charge density was Fourier expanded up to G_{max} =12. K ($1s^2\ 2s^2\ 2p^6$), Cl ($1s^2$

$2s^2\ 2p^6$) and Cu ($1s^2\ 2s^2\ 2p^6\ 3s^2$) electronic states are treated as core states, and K ($3s^2\ 3p^6\ 4s^1$), Cl ($3s^2\ 3p^5$) and Cu ($3p^6\ 3d^{10}\ 4s^1$) are considered valence states. For the KCl lattice, a self-consistent procedure was performed on a grid containing 10 × 10 × 10 **k** points in the First Brillouin Zone (FBZ), i.e., the Irreducible Brillouin Zone (IBZ) was sampled on a tetrahedral mesh with 47 **k** points. For the KCl:Cu lattice, the calculations were performed using a grid containing 3 × 3 × 3 **k** points in the FBZ, sampling the IBZ on a tetrahedral mesh with 4 **k** points.

For the calculations of the optical properties, the WIEN2k program *optic* was used. The Independent Particle Random Phase Approximation (RPA) is assumed and local field effects are not included [32]. The momentum matrix elements are calculated from the electron states, and the integration over the IBZ is performed to calculate the imaginary part of the dielectric function ε_2 [33,34]. A Kramers-Kronig analysis is performed to obtain the real part of the dielectric function ε_1, and finally, the absorption spectra are calculated from this complex dielectric function. In the present study of optical properties, we only take into account the electric-dipole allowed interband transitions and neglect the *d-d* transitions. The primary quantity that characterizes the electronic structure of any crystalline material is the probability of photon absorption, which is directly related to the imaginary part of the dielectric function ε_2. Thus, this function can be associated with interband transitions providing information about single particle excitation, i.e., the peaks observed in this function can be related to electronic transitions in the crystalline material. The real part ε_1 provides information about collective electronic excitations (plasmons) in the system, obtaining the plasmon energy at points where ε_1 crosses zero with a positive slope.

3. Results and discussion

3.1. Structural properties

In order to verify our computational parameters, we firstly optimized the lattice parameter of KCl, using WIEN2k with the PBE96 exchange-correlation energy functional. For this, we calculate the total energy of the cubic lattice for different volume values (varying the parameter *a*). Fitting our calculated data with the Murnaghan equation of state [35], we obtain a value of $a = 6.384$ Å for the lattice parameter, which overestimates the experimental value by 1.45 % [24]. For the KCl:Cu supercell optimization, we compute both the atomic positions and the cell volume that minimize the internal forces and total energy, respectively. First, we calculate the atomic positions minimizing the internal forces acting on the atoms. To this, an internal relaxation of the atoms is performed by varying the positions of the K and Cl atoms surrounding the Cu atoms, and the total forces exerted on each atom are calculated. The system is relaxed until the total forces are below 1.0 mRy/a.u. This internal relaxation produced a reduction of the distance Cu-Cl, compared with the K-Cl distance of the pristine crystal. Similarly, the distance of the nearest K atoms to Cu ones also decreased, thus causing a distortion of the lattice around Cu atoms. This behavior is expected, given the smaller size of Cu ion regarding that of the K ion. After relaxation of the internal positions, we calculate the total energy versus lattice volume curve, varying the lattice parameter of the supercell. Fitting our calculated values to the Murnaghan equation [35], we obtain the optimized supercell lattice parameter a = 19.117 Å.

3.2. Electronic properties

3.2.1. Energy band structures

To analyze the *k*-resolved information of KCl and KCl:Cu compounds, we utilized the modified Becke-Johnson (mBJ) exchange potential in combination with the local density approximation (LDA) for correlation, as suggested by Tran and Blaha [29]. we calculate the energy band structures using the atomic positions and the optimized cell parameters. For KCl, the band structure is obtained along the lines connecting the high-symmetry points in the reciprocal space shown in Fig. 2(a). This figure displays an insulator behavior of the pure crystal, with a direct band gap of 8.6 eV at **Γ** point. This is in excellent agreement with the experimental values reported by Phillips [36], and Roessler and Walker [37] at **Γ** point (8.69 and 8.5 eV, respectively). Bands with low dispersion are observed at -12.2, -11.0 and 0.0 eV. The Fermi level is indicated by a horizontal line at 0.0 eV, separating the valence band (VB) from the conduction band (CB), which are located above 8.6 eV. Analyzing the band character, the bands at -12.2 and -11.0 eV are constituted by Cl *s* and K *p* states, respectively. At the Fermi level the bands correspond to Cl *p* states, and the unoccupied K *d* states conform the conduction bands, principally. This is in agreement with the analysis presented by Roessler and Walker [37]. Recently, Bahattin et al. [38] calculated the band structure of KCl with the ABINIT code using the PBE96 approximation. In the current work, the overall shape of the calculated band structure compares quite well with that obtained by Bahattin et al. [38]. In Table 1 we present the calculated transition energy values at different reciprocal space points, which are compared with experimental values presented in [36,37]. Our results show a good agreement with the available experimental information.

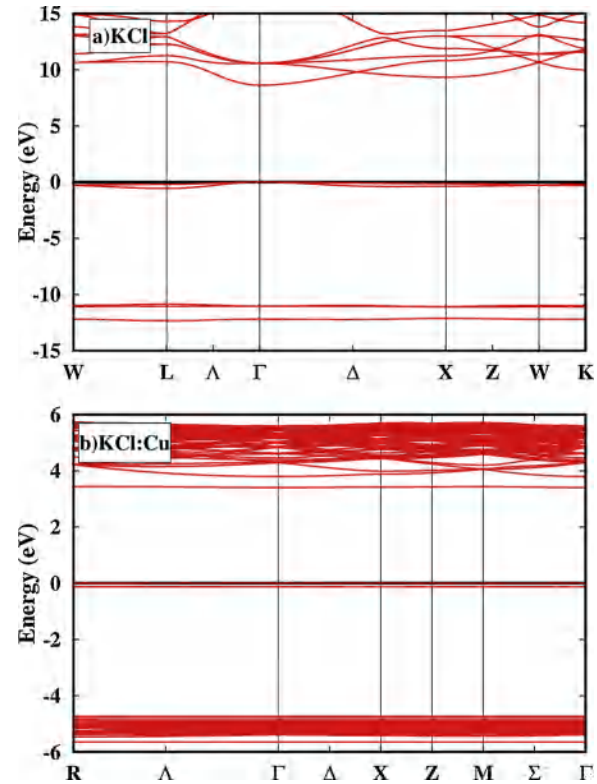

Fig. 2. Calculated band structures of (a) KCl and (b) KCl:Cu. The Fermi level is shifted at 0.0 eV.

For KCl:Cu, energy bands are plotted in Fig. 2(b) for different high-symmetry points in the reciprocal space, ranging from **R**(1/2,1/2,1/2) to **Γ**(0,0,0) to **X**(1/2,0,0) to **M**(1/2,1/2,0) to **Γ**(0,0,0). Examining this figure, it is observed that no bands cross the Fermi level, which suggests a non-metallic behavior and reveals the existence of a band gap. This direct band gap is found at the **Γ** point with a calculated value of 3.4 eV. It is also evident the dispersionless character of the band structure, which shows the existence of localized states. These are reflected in the existence of sharp peaks in the density of states, in particular around the region of the Fermi energy. In this compound, the band character near the Fermi level is dominated by Cu *d* states, while the flat band at 3.4 eV is constituted by Cu *s* states. These new bands are introduced as an effect of doping of the KCl lattice with Cu atoms. Also, the bands above

Table 1
Comparison of the calculated energy values of selected KCl band transitions with experimental data. Band transitions nomenclature is taken from [37].

Band Transition	Energy (eV) (a)	(b)	This work
$\Gamma_{15} \rightarrow \Gamma_1$	8.69	8.5	8.62
$L_3 \rightarrow L_2'$	9.0	10.35, 10.45	10.90
$\Lambda_3 \rightarrow \Lambda_1$ (LAMBDA)	9.2	–	9.67
$X_5' \rightarrow X_1$	10.9	13.7	10.81
$\Delta_5 \rightarrow \Delta_1$	11.1	–	9.72
$X_5' \rightarrow X_3$	9.9	12.6	9.43
$L_3 \rightarrow L_3'$	11.2	–	11.24
$\Gamma_{15} \rightarrow \Gamma_{25}'$	11.6	–	10.55

(a) See reference [37].
(b) See reference [36].

3.8 eV are mostly constituted by K *d* states and the bands around -5.0 eV primarily by Cl *p* states. The low dispersion of bands at -5.0, 0.0 and 3.4 eV is representative of a relatively high concentration of electrons corresponding to Cl *p*, Cu *d*, and Cu *s* states, respectively.

3.2.2. Total and projected density of states

To elucidate the atomic electronic contributions to the electronic structure of KCl and KCl:Cu crystals, we calculate and examine in detail the corresponding total and partial density of states (DOS and PDOS, respectively). For KCl (Fig. 3), our results show that at the Fermi level (0.0 eV) the main contribution to DOS arise from Cl p states, whereas the Cl s and K p states are well below the Fermi level (12 and 11 eV, respectively). The conduction states start to appear at 8.6 eV above Fermi energy, which mainly result from the K d states. Our calculated DOS is similar to that calculated by Bahattin et al. [38], but as mentioned before, they underestimate the energy gap. Our calculated band gap is of 8.6 eV, in close agreement to the reported experimental value [36,37]. Fig. 4 depicts the DOS and PDOS results of KCl:Cu, showing the principal contributions of Cu, K and Cl states to the DOS. The peaks around -5.0 eV are mainly formed by Cl states, specifically p states, the peaks at the Fermi level arise from Cu d states, and the strong peak at 3.4 eV has mainly Cu s character with minor contributions from states between 3.8 and 5.0 eV (see inset in Fig. 4). Above 5.0 eV, this figure also reveals contributions to the conduction states from K, Cl, and Cu atoms (PDOS in gray). Likewise, it is observed that the peak structure of the DOS for KCl is present in the DOS of KCl:Cu, with additional states within the band gap of KCl, which are associated to the doping Cu atoms.

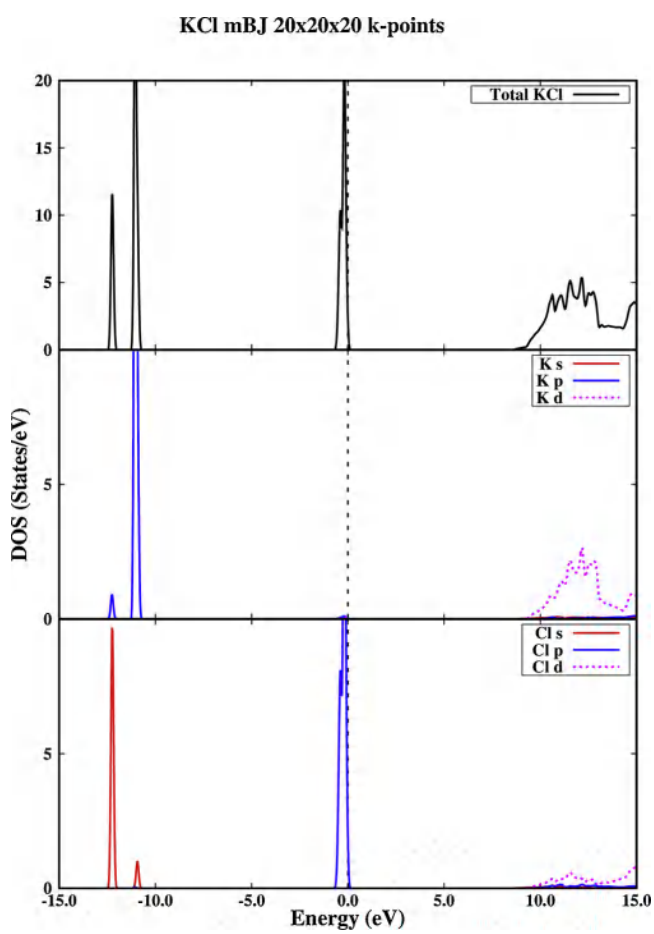

Fig. 3. Calculated total and partial density of states (PDOS) of KCl using mBJ approximation. The Fermi energy is shifted at 0.0 eV.

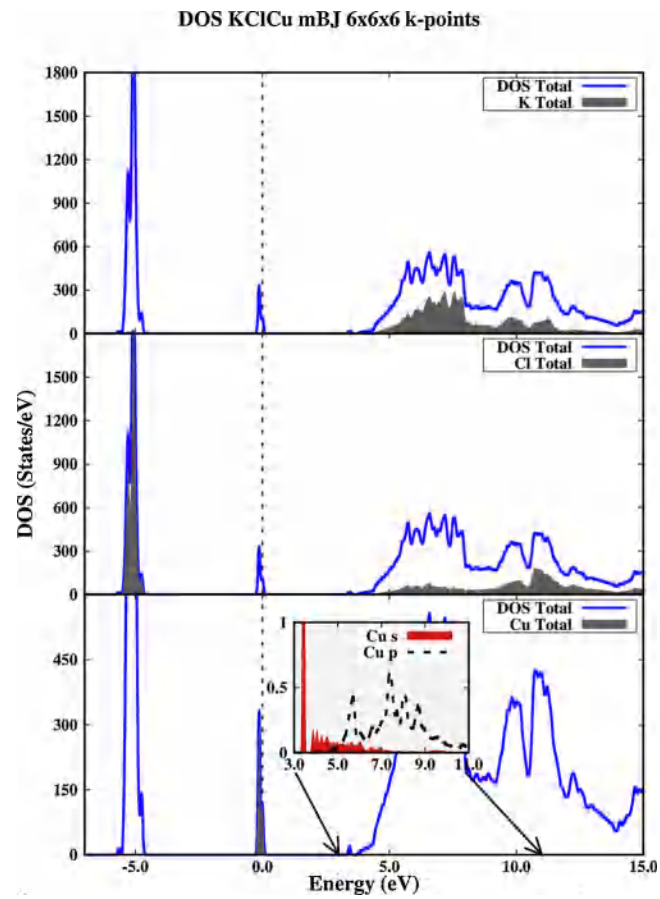

Fig. 4. Total density of states of KCl:Cu (blue line) and the total contribution to DOS from (a) K, (b) Cl, and (c) Cu atoms (shaded in gray). The inset shows the contribution of Cu *s* and *p* states to empty valence states above the Fermi level. (For interpretation of the references to colour in this figure legend, the reader is referred to the web version of this article).

3.3. Optical properties

The aim of this section is to examine the optical properties of both, pristine and Cu-doped KCl. To this end, the real (ε_1) and imaginary (ε_2) parts of the dielectric function are computed (Fig. 5), as well the absorption spectra (Fig. 6). The overall shape of the calculated optical properties (Figs. 5 and 6) for KCl and KCl:Cu are quite similar, except for the peaks shifting left towards lower energy values, by about 0.1 eV, of the KCl:Cu system regarding those of the pure KCl compound. Also, a small peak at about 8.17 eV appears in the KCl:Cu spectrum (Fig. 5(b)).

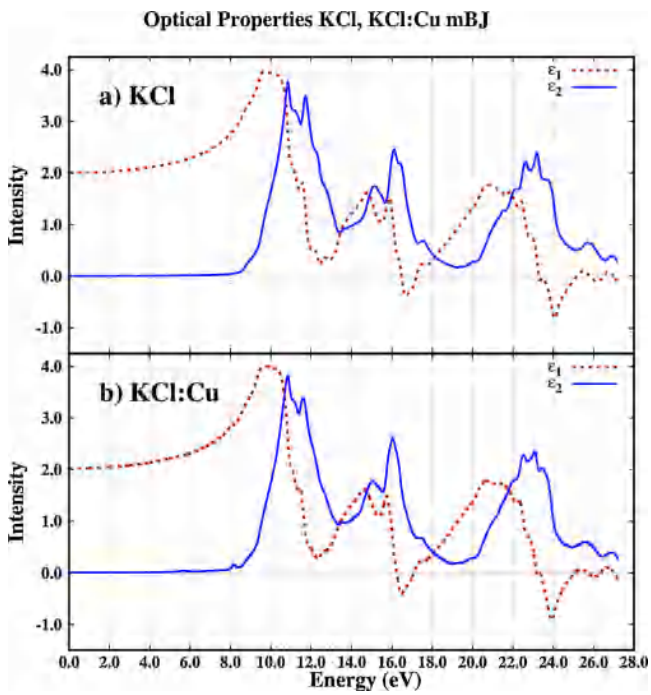

Fig. 5. Dielectric function of KCl and KCl:Cu, calculated using the TB-mBJ functional.

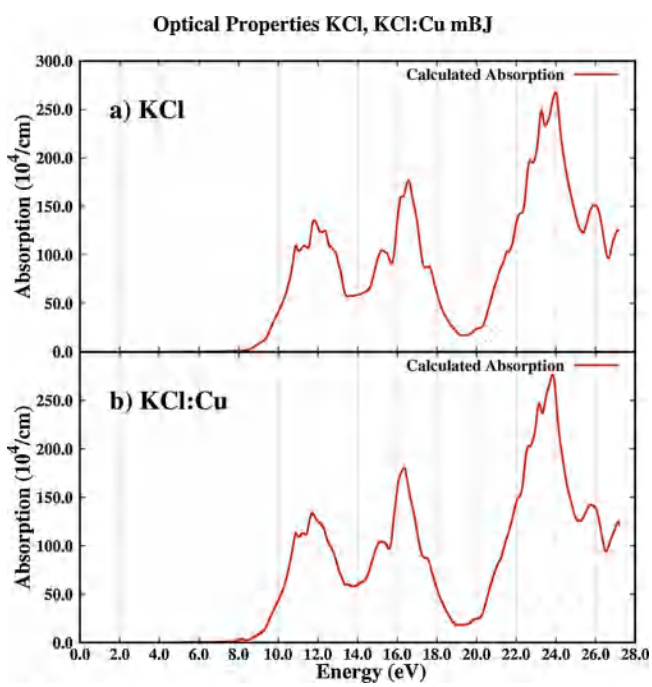

Fig. 6. Calculated optical absorption as a function of energy for KCl and KCl:Cu, using TB-mBJ approximation.

This feature is reproduced in Fig. 6(b), thus attributing this peak to the Cu doping of KCl, i.e., to contributions from a number of Cu states to the conduction band. With the aim of understanding the origin of this peak, a closer look on the calculated absorption spectrum of the doped KCl crystal is necessary. Therefore, the absorption spectrum is calculated and examined in a much narrower range of energies. In Fig. 7 we show the optical absorption spectrum for KCl and KCl:Cu within an energy range between 3 and 9 eV. Interestingly, for the doped crystal, our analysis shows the existence of two peaks appearing at 5.7 and 8.17 eV, and two more small peaks revealed at about 6.8 and 7.4 eV. Thus,

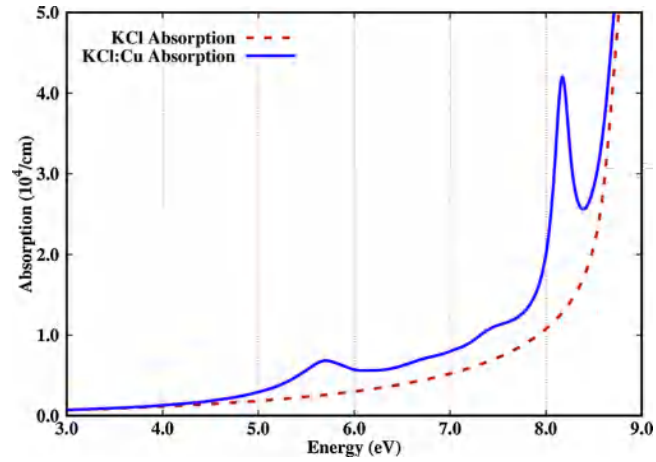

Fig. 7. Calculated absorption spectra of KCl and KCl:Cu, depicted in an energy range below 9 eV.

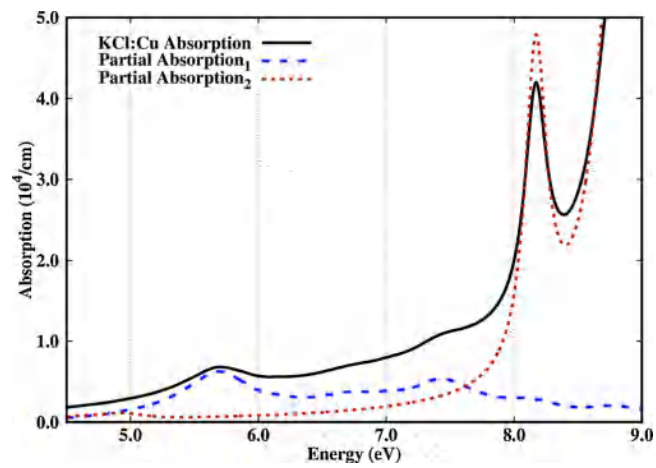

Fig. 8. Calculated total and partial absorptions spectra of KCl:Cu. These partial absorptions are calculated considering only transitions between energy bands in a reduced energy range (see optical properties, section 3.3).

these additional peaks are also related to interband transitions involving Cu states. From an analysis of the partial absorption spectrum of KCl:Cu (see Fig. 8, partial absorption 1) related to bands at the Fermi level and above (up to 14.21 eV), it exhibits peaks at 5.7, 6.8, and 7.4 eV, which correspond to electron transitions between valence bands with Cu *d* character to conduction bands with *p* character of Cl, K and Cu. The peak at 8.17 eV is obtained by calculating the partial absorption spectrum involving bands in the range of energies -5.65 to 5.0 eV (see Fig. 8, partial absorption 2). This peak arises from transitions between bands with Cl *p* character and the first conduction band with Cu *s* character. Also, in this region of energy a small peak is observed at about 4.9 eV, this is a truncated peak due to the limited range of energies considered, and can be assigned to transitions between bands with Cu *d* character to conduction bands with *p* character.

Comparing our results with experimental information, our calculated ε_2 function for KCl reproduces quite well the experimental data published in [37]. They obtain a wide peak between 10 and 14 eV in the ε_2 function produced by interband transitions, while our calculated ε_2 function shows a wide structure between 9.0 and 14.0 eV. The comparison with data beyond 14 eV is not good, but in this work it is commented an increase in ε_2 beyond 16 eV because of transitions between valence and conduction bands, which we also observe. For KCl:Cu, Oggioni and Scaramelli [39] report three peaks below 6.5 eV in the absorption spectra of KCl:Cu, at about 4.79, 5.37, and 6.093 eV (259, 231, and 203.5 nm, respectively). The absorption at 4.79 eV is

attributed to the forbidden transition Cu *d* - Cu *s* of isolated Cu ion, while the absorption at 5.37 and 6.093 eV are attributed to optical transitions of Cu ion from the ground state to higher excited states. These latter peaks are apparently related to our calculated peaks at about 5.7 and 6.76 eV which are due to Cu *d* electron transitions from the valence band to bands with *p* character of Cl, K and Cu in the conduction band.

4. Conclusions

A detailed analysis of the electronic and optical properties of KCl and KCl:Cu has been performed through density functional theory, utilizing two different exchange-correlation functionals, PBE96 and a combination of mBJ (exchange) and LDA (correlation) functionals. From the calculated energy band structure and density of states, an insulating behavior is predicted for KCl with a direct band gap of 8.6 eV at **Γ** point, a value very close to the experimental result, while a semiconductor behavior is obtained for KCl:Cu, with a direct band gap of about 3.4 eV at **Γ** point. For KCl the valence states at the Fermi level correspond to Cl *p* orbitals, while conduction states arise from K *d* orbitals. For KCl:Cu, the valence states arise from Cu *d* orbitals, and conduction states result mainly from K *d* orbitals. Our results show that new states emerge in the band gap of KCl when Cu atoms are incorporated into the KCl lattice.

From the calculated optical properties, the optical absorption properties of KCl are modified below 9.0 eV as an effect of Cu doping. In this range, KCl:Cu shows new peaks in the calculated absorption spectra, which are ascribed to several interband transitions. From an analysis of the partial absorption spectra we determine that peaks at 5.7, 6.8, and 7.4 eV are related to band transitions with Cu *d* and Cu *p* character, and the peak at 8.17 eV is due to electronic transitions between bands with Cl *p* and Cu *s* character. Thus, our results support that the $3d^{10} \rightarrow 3d^{9}4p$ transition gives rise to the three absorption peaks below 7.4 eV.

Data availability

The data required to reproduce these findings can be obtained by contacting the corresponding author.

Declaration of Competing Interest

The authors declare that they have no known competing financial interests or personal relationships that could have appeared to influence the work reported in this paper.

Acknowledgements

The authors are grateful to ACARUS at Universidad de Sonora for the computer time support. A.P.A acknowledges Conacyt for funding project 180424.

References

[1] K. Fussaenger, On the UV absorption of heavy metal ions in alkali halide crystals, Phys Stat Sol 34 (1969) 157.
[2] H. Chermette, C. Pedrini, MSX□ calculation of adiabatic potential energy surfaces of Cu+ in sodium chloride lattice in the a_{1g} subspace. Incidence of the copper-chlorine distance of the electronic structure, J. Chem. Phys. 77 (1982) 2460–2465.
[3] N.W. Winter, R.M. Pitzer, D.K. Temple, Hartree-Fock calculation of the electronic structure of a Cu+ impurity in NaCl, J. Chem. Phys. 87 (1987) 2945–2953.
[4] J. Simonetti, D.S. McClure, The 3d→4p transition of Cu^{+} in Cl and of transition-metal ions in crystals, Phys. Rev. B 16 (1977) 3887–3892.
[5] W.E. Hagston, Theory of the fine structure of the UV absorption of heavy metal ions in the alkali halides, J. Phys. C.: Solid State Phys. 5 (1972) 691–701.
[6] Stephen A. Payne, Analysis of the off-center effect of Cu+ in alkali halides using crystal-field theory, Phys. Rev. B 36 (1987) 6125–6131.
[7] M. Furukuya, S. Ishii, Y. Takahashi, S. Nagasaka, T. Yoshinari, Y. Kawazoe, K. Ohno, Stability of copper atoms embedded in sodium-chloride crystals, Mater. Trans. 45 (5) (2014) 1450–1451.
[8] M.S. Holston, I.P. Ferguson, N.C. Giles, J.W.- McClory, D.J. Winarski, J. Ji, F.A. Selim, L.E. Halliburton, Green Luminescence from Cu-diffused $LiGaO_2$crystals, J. Lumin. 170 (2016) 17–23.
[9] V. Yerpude, S. Tamboli, K.B. Ghormare, S.J. Dhoble, Optical properties of Cu+ ions activated $Na_2Zn(PO_4)Cl$ phosphor, J. Optoelectron. Adv. M. 20 (11–12) (2018) 651–656.
[10] B. Capoen, H.E. Hamzaoui, M. Bouazaoui, Y. Ouerdane, A. Boukenter, S. Girard, C. Marcandella, O. Duhamel, Sol-gel derived copper-doped silica glass as a sensitive material for X-ray dosimetry", Opt. Mater. (Amst) 51 (2016) 104–109.
[11] N.A. Helou, H.E. Hamzaoui, B. Capoen, Y. Ouerdane, A. Boukenter, S. Girard, M. Bouazaoui, Effects of ionizing radiation on the optical properties of ionic copper-activated sol-gel silica glasses, Opt. Mater. (Amst) 75 (2018) 116–121.
[12] H.E. Hamzaoui, Y. Ouerdane, L. Bigot, G. Bouwmans, B. Capoen, A. Boukenter, S. Girard, M. Bouazaoui, Sol-gel derived ionic copper-doped microstructured optical fiber: a potential selective ultraviolet radiation dosimeter, Opt. Express 20 (28) (2012) 29751.
[13] S. Girard, B. Capoen, H. El Hamzaoui, M. Bouazaoui, G. Bouwmans, A. Morana, D. Di Francesca, A. Boukenter, O. Duhamel, P. Paillet, M. Raine, M. Gaillardin, M. Trinczek, C. Hoehr, E. Blackmore, Y. Ouerdane, Potential of copper- and cerium-doped optical Fiber materilas for proton beam monitoring, IEEE Trans. Plasma Sci. IEEE Nucl. Plasma Sci. Soc. 64 (1) (2017) 567–573.
[14] T. Rivera, L. Olvera, A. Martínez, D. Molina, J. Azorín, M. Barrera, A.M. Soto, R. Sosa, C. Furetta, Thermoluminescence properties of copper doped Zirconium oxide for UVR dosimetry, Radiat. Meas. 42 (2007) 665–667.
[15] I. Aguirre de Carcer, V. Correcher, M. Barboza-Flores, H.L. D'Antoni, F. Jaque, Preliminary results on the identification of ultraviolet and beta radiation exposure in KCl:Eu2+ single crystals by thermoluminescence, Nucl. Instrum. Methods Phys. Res. B 267 (2009) 2870–2873.
[16] I. Aguirre de Carcer, H.L. D'Antoni, M. Barboza-Flores, V. Correcher, F. Jaque, KCl:Eu2+ as a solar UV-Cradiation dosimeter. Optically stimulated luminescence and thermoluminescence analyses, J. Rare Earth 27 (4) (2009) 579–583.
[17] A.L. Huston, B.L. Justus, P.L. Falkenstein, R.W. Miller, H. Ning, R. Altemus, Remote optical fiber dosimetry, Nucl. Instr. Meth. Phys. Res. 184 (2001) 55–67.
[18] M.S. Holston, I.P. Ferguson, N.C. Giles, J.W. McClory, L.E. Halliburton, Identification of defects responsible for optically stimulated luminescence (OSL) from copper-diffused $LiAlO_2$ crystals, J. Lumin. 164 (2015) 105–111.
[19] P.K. Bandyopadhyay, G.W. Russell, K. Chakrabarti, Optically Stimulated luminescence in KCl:Cu x-irradiated at room temperature, Radiat. Meas. 30 (1999) 51–57.
[20] Z.J. Chen, H.Y. Xiao, X.T. Zu, First principles study of structural, electronic and optical properties of KCl crystal, Chem. Phys. 300 (2006) 1–8.
[21] A. Myasnikova, A. Mysovsky, A. Paklin, A. Shalaev, Structure and optical properties of copper impurity in LiF and NaF crystals from ab initio calculations, Chem. Phys. Lett. 633 (2015) 218–222.
[22] Y.K. Sun, J.H. Zhang, J.W. Ding, X.H. Yan, First-principles study on electronic and optical properties of Cu-doped LiF with Li vacancy, Physica B 407 (2012) 2458–2461.
[23] C. Kittel, Introduction to Solid State Physics, 7th ed., Wiley, 1996.
[24] Georg K.H. Madsen, Peter Blaha, Karlheinz Schwarz, Elisabeth Sjöstedt, Lars Nordström, Efficient linearization of the augmented plane-wave method, Phys. Rev. B 64 (2001) 195134.
[25] P. Hohenberg, W. Kohn, Inhomogeneous Electron gas, Phys. Rev. B136 (1964) 864.
[26] W. Kohn, L.J. Sham, Self-consistent equations including exchange and correlation effects, Phys. Rev. A140 (1965) 1133.
[27] P. Blaha, K. Schwarz, G.K.H. Madsen, D. Kvasnicka, J. Luitz, WIEN2k, An Augmented Plane Wave Plus Local Orbitals Program for Calculating Crystal Properties, Vienna University of Technology, Vienna, Austria, 2001.
[28] J.P. Perdew, S. Burke, M. Ernzerhof, Generalized gradient approximation made simple, Phys. Rev. Lett. 77 (1996) 3865.
[29] F. Tran, P. Blaha, Accurate band gaps of semiconductors and insulators with a semilocal exchange-correlation potential, Phys. Rev. Lett. 102 (2009) 226401.
[30] D. Koller, F. Tran, P. Blaha, Improving the modified Becke-Johnson exchange potential, Phys. Rev. B 85 (2012) 155109.
[31] A.D. Becke, E.R. Johnson, A simple effective potential for exchange, J. Chem. Phys. 124 (2006) 221101.
[32] C. Ambrosch-Draxl, J.O. Sofo, Linear Optical Properties of Solids Within the Full-potential Linearized Augmented Planewave Method, arXiv:cond-mat/0402523, (2004).
[33] R. Del Sole, R. Girlanda, Optical properties of semiconductors within the independent-quasiparticle approximation, Phys. Rev. B 48 (1993) 11789.
[34] C. Ambrosch-Draxl, J.A. Majewski, P. Vogl, G. Leising, First-principles studies of the structural and optical properties of crystalline poly(para-phenylene), Phys. Rev. B 51 (1995) 9668.
[35] F.D. Murnaghan, The compressibility of media under extreme pressures, Proc. Natl. Acad. Sci. U.S.A. 30 (1944) 244–247.
[36] J.C. Phillips, Ultraviolet Absorption of Insulators. III. fcc Alkali Halides, Phys. Rev. 136 (1964) A1705.
[37] D.M. Roessler, W.C. Walker, Electronic spectra of crystalline NaCl and KCl, Phys. Rev. 166 (1968) 599.
[38] B. Erdinc, M.N. Secuk, M. Aycibin, S.E. Gülebagan, E.K. Dogan, H. Akkus, Ab-initio calculations of physical properties of alkali chloride XCl (X = K, Rb and Li) under pressure, Comp. Cond. Matt. 4 (2015) 6–12.
[39] R. Oggioni, P. Scaramelli, Optical absorption and photoluminescence of Cu-doped alkali halide crystals, Phys Stat Sol 9 (1965) 411–421.